Miscibility of Poly(*n*-butyl acrylate)/Poly(propylene glycol) Blends. 1. Phase Behavior and Dielectric Relaxation

Tadashi Hayakawa† and Keiichiro Adachi*

Department of Macromolecular Science, Graduate School of Science, Osaka University, Toyonaka, Osaka 560-0043, Japan

Received April 19, 2000

ABSTRACT: We report the cloud point, glass transition temperature T_g, and dielectric relaxation for blends composed of poly(*n*-butyl acrylate)s (PBA) and a linear poly(propylene glycol) (PPGD) and for blends of PBA and a star-shaped PPG having three arms (PPGT). The phase diagram is of the upper critical solution type (UCST), and the critical temperature varies from 340 to 220 K depending on the molecular weight of the PBA. The interaction parameter χ for PBA/PPGD is higher than that for PBA/PPGT. For blends of high molecular weight PBA and PPGD, a sharp glass transition and a subsequent broad glass transition were observed by differential scanning calorimetry, but for mixed blends a relatively sharp single T_g was observed. The temperature dependence of the dielectric loss factor ϵ'' of phase-separated blends exhibited two loss maxima. The low-temperature peak can be assigned to the segmental mode relaxation (α-process) of PPG and the high-temperature peak to the normal mode of PPG and the segmental mode of PBA. Mixed blends exhibited a single loss maximum having an asymmetrical shape, indicating that there is local heterogeneity.

Introduction

Polymer blends have been used widely since they often have physical properties superior to the component polymers.[1] Since the properties depend strongly on the miscibility of the components, the miscibility of polymer blends has been studied with various methods,[2] such as calorimetry,[3,4] cloud point measurements,[5−8] dynamic mechanical relaxation,[9] NMR,[10] electron microscopy,[11] and the dielectric method.[12−17] In an apparently homogeneous blend composed of polymers 1 and 2, there exist 1-rich and 2-rich regions, and the dimension of the heterogeneity is characterized by the correlation length.[17] The correlation length is expected to increase near the phase separation temperature. Therefore, the phase diagrams of blends have been studied by many authors.[5−8] A well-known phase diagram of a polymer blend is that for polystyrene (PS) and poly(vinyl methyl ether) (PVME) reported first by Nishi et al.[18]

In the present article we report the cloud points of blends composed of poly(*n*-butyl acrylate)s (PBA) and poly(propylene glycol)s (PPG). We used a linear PPG (PPGD) and a star-shaped PPG with three arms (PPGT). Only a few studies are reported on the effect of branching on the miscibilities of polymers.[19] Faust et al.[19] reported the miscibility of a star-shaped PS with 22 arms and a linear PVME. They reported that the lower critical solution temperature (LCST) for the linear/linear blend is the same as that for the star/linear blend, but the shapes of the binodal curves are different. If the Flory−Huggins theory[20,21] predicts correctly the phase separation behavior of a polymer blend, the phase behavior will be independent of the architectures of the components. We report here the effect of the star-shaped branching on the phase behavior of PBA/PPG blends.

When a blend composed of polymers 1 and 2 is demixed, two glass transition temperatures T_g of the components will be observed. But an ideally mixed blend exhibits a single glass transition T_g at an intermediate temperature between the T_g's of the components.[2−4] This has long been used as the criterion of miscibility of blends. Similar behavior can be observed by dielectric or mechanical measurements; i.e., a demixed blend exhibits two loss peaks due to the segmental relaxations (α relaxation) of the components, but an ideally mixed blend exhibits a single loss peak.[2,9,12−17] In real blends, we expect that the dielectric relaxation spectra will be intermediate between those two extreme cases and exhibit a variety of patterns depending on the difference between the cloud point and the temperature at which the relaxation is observed. Besides the segmental mode, PPG exhibits a weak dielectric normal mode relaxation due to fluctuation of the end-to-end distance, which was first reported by Stockmayer and co-workers.[22−25] Recently, Se et al. reported the effect of miscibility on the normal mode relaxation of *cis*-polyisoprene (*cis*-PI) in blends containing *cis*-PI.[17] In this paper we also report the behavior of the normal mode of PPG in the blends. Our second objective is to examine the glass transition and dielectric behavior of PBA/PPG blends.

Experimental Section

Materials. A high molecular weight poly(*n*-butyl acrylate) (PBA) sample was purchased from Aldrich Chemical Co. Inc. A low molecular weight PBA was supplied from Nippon Shokubai Co., Ltd. (Osaka, Japan). As they had very broad distributions of molecular weight, fractionation of these PBA samples was carried out by adding methanol to 1−0.1 wt % tetrahydrofuran (THF) solutions. Narrow distribution samples (PBA-5 and PBA-3) were purchased from Polymer Source, Inc. (Dorval, Canada).

Linear and star-shaped three arm PPG samples were purchased from Mitsui Chemicals Inc. (Tokyo, Japan) For the PBA samples M_w was determined by gel permeation chromatography (GPC) by using an apparatus equipped with a low-angle laser light scattering detector (Tosoh LS8000, Tokyo, Japan). The carrier solvent was THF. Commercially available narrow molecular weight distribution polystyrenes were used as the standard of light scattering.

† Present address: Nippon NSC Co., 1-6-5 Senba-nishi, Minou, Osaka 562-8586, Japan.

* To whom correspondence should be addressed.

10.1021/ma000684v CCC: $19.00
Published on Web 08/12/2000

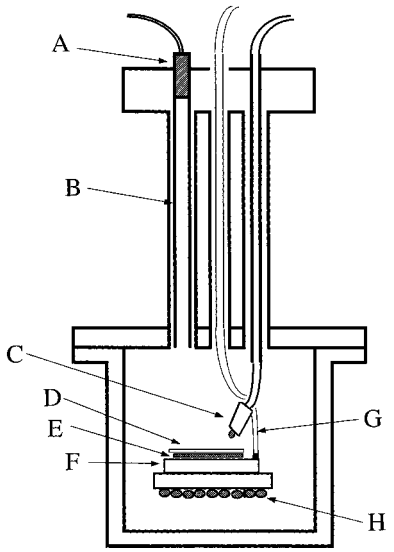

Figure 1. Schematic diagram representing the measurements of the cloud point: (A) semiconductor laser; (B) guide of laser beam; (C) photodiode; (D) thin glass plate; (E) sample; (F) mirror; (G) thermocouple; (H) heater.

Table 1. Characteristics of Sample Polymers

code	$10^{-3}M_w$	M_w/M_n	T_g/K
PBA-380	380	1.38	222
PBA-240	242	1.44	223
PBA-42	42	1.20	223
PBA-21	21	1.27	225
PBA-5	5.4	1.13	
PBA-3	3.0	1.20	211
PPGD-3	2.9	1.10	201
PPGT-6	5.9	1.10	201

The number-average molecular weight of PPG was determined by end group analysis with ^{13}C NMR (JPEL Lambda 500, Tokyo, Japan). The ratio of intensities of $^{13}C-OH$ and the methylene carbons was determined with a precaution about the T_1 effect. For all samples M_w, M_n, and M_w/M_n are listed in Table 1. The blends were prepared by dissolving the constituent polymers in THF so that the components were well mixed, and then the solvent was evaporated completely under 0.01 Torr at 80 °C.

Method. Measurement of turbidity was made by using an apparatus shown in Figure 1. A small amount of a PBA/PPG blend was put on a mirror and covered by a thin glass plate. The sample was set on the sample holder as shown in Figure 1 and was irradiated by semiconductor laser light of ca. 2 mW with wavelength of 610 nm (Japan Laser Co. MLX-D12, Tokyo, Japan). When the sample was in a mixed state, the scattered light was weak, while for a phase-separated state the scattered light became intense. Such a change was detected by a photodiode (Hamamatsu Photonics, S1190, Shizuoka, Japan). The measurements were carried out with a heating rate of ca. 2 °C/min in the heating direction from about 185 K. Dielectric measurements were carried out with an RLC digibridge (QuadTech 1693, Maynard, MA). The dielectric cell for measurements of viscous polymer samples was described previously.[26] Measurements of T_g were made with a differential scanning calorimeter (Seiko, SSC580, Tokyo, Japan).

Results and Discussion

Figure 2 shows the phase diagrams of two blends of PBA and linear PPG: PBA-240/PPGD-3 and PBA-42/PPGD-3. As shown in Figure 2, these phase diagrams exhibit upper critical solution temperatures (UCST). The UCSTs of PBA-240/PPGD-3 and PBA-42/PPGD-3 were 280 and 261 K, respectively. The PBA content ϕ_c of PBA-240/PPGD-3 at the UCST was 0.20 ± 0.05, and ϕ_c of PBA-42/PPGD-3 was 0.24 ± 0.02.

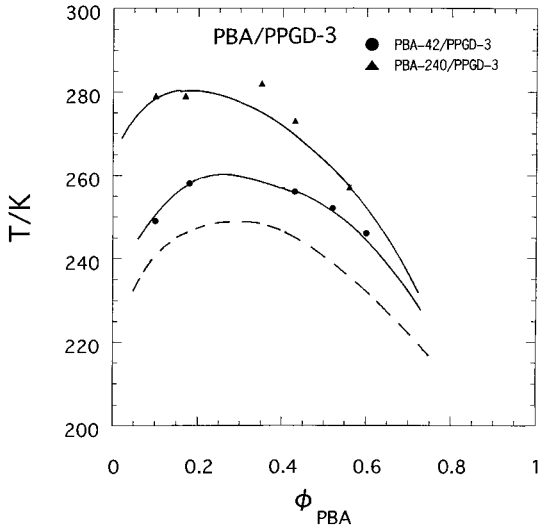

Figure 2. Cloud points of blends of PBA-240/PPGD-3 (filled triangle) and PBA-42/PPGD-3 (filled circle). Dashed line indicates the cloud point of PBA-21/PPGD-3 calculated with the F−H theory by using the χ parameter given in Table 2.

According to the Flory−Huggins (F−H) theory, the free energy of mixing ΔG of two polymers 1 and 2 is given by[20,21]

$$\Delta G = \frac{RTV}{v_c}\left(\frac{\phi_1}{x_1}\ln\phi_1 + \frac{\phi_2}{x_2}\ln\phi_2 + \chi\phi_1\phi_2\right) \qquad (1)$$

where V is the volume of the system, v_c the volume of the unit cell of the lattice model, ϕ_j the volume fraction, x_j the degree of polymerization in terms of the unit v_c, and χ the interaction parameter. We take the monomeric unit of PBA as the reference unit. Then we need to determine the molecular weight of PPG per unit cell. We expect that ca. two monomeric units of PPG correspond to the F−H lattice unit and determined the molecular weight of the unit as follows. From the condition that the third derivative of ΔG with respect to ϕ vanishes at the critical point, the volume fraction ϕ_c at the critical point is given by

$$\phi_c = \frac{\sqrt{x_2}}{\sqrt{x_1}+\sqrt{x_2}} \qquad (2)$$

From the data of $\phi_c = 0.24$ for PBA-42/PPGD-3, and that the degree of polymerization $x_1 = 326$ of PBA-42, we determined x_2 corresponding to the number of the F−H unit of PPGD-3 to be 33. This corresponds to the molecular weight of the unit cell of 88. Since the molecular weight of PPG monomer unit is 58, the F−H unit contains approximately 1.5 PPG monomeric units.

The interaction parameter χ is often given by the form

$$\chi = \alpha + \frac{\beta}{T} \qquad (3)$$

where T is the temperature and α and β are parameters. According to the F−H equation,[7] the value of χ at T_c (χ_c) of a blend is given by

$$\chi_c = \frac{1}{2}\left(\frac{1}{\sqrt{x_1}} + \frac{1}{\sqrt{x_2}}\right)^2 \qquad (4)$$

From two values of T_c for the PBA/PPGD-3 blends, we

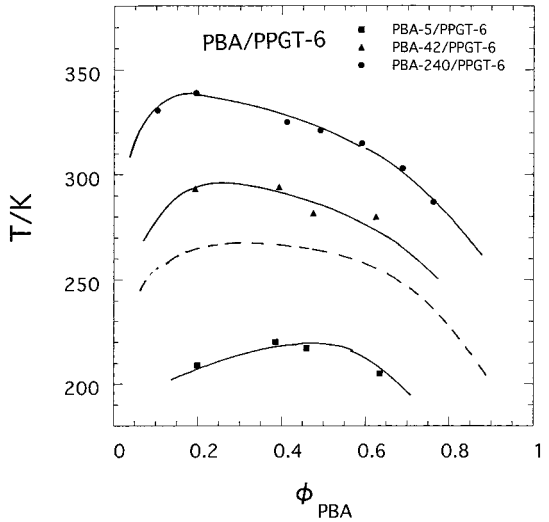

Figure 3. Cloud points of blends of PBA-240/PPGT-6 (circle), PBA-42/PPGT-6 (triangle), and PBA-5/PPGT-6 (square). Dashed line indicates the cloud point of PBA-21/PPGT-6 calculated with the F−H theory.

Table 2. Conatant α and β of Interaction Parameters

blends	α	β
PBA/PPGD-3	−0.075	27
PBA/PPGT-6	−0.027	13

determined the constants of α and β to be −0.075 and +27, respectively. Equation 4 holds only when χ is independent of the composition. Therefore, the α and β values determined above are only approximate. Using these parameters, we calculated the phase diagram from the free energy of blending ΔG. The common tangential line was drawn for the ΔG versus ϕ curve at a particular temperature, and two binodal compositions at the temperature were determined. The binodal curves thus calculated are indicated by the solid and dashed lines in Figures 2 and 3. The determination of the binodal compositions becomes difficult near the critical temperature since the ΔG curve does not exhibit clear concave and convex. Therefore, the phase separation temperatures thus determined are approximate values.

Figure 3 shows the phase diagrams of three combinations of PBA and star-shaped PPG, i.e., PBA-240/PPGT-6, PBA-42/PPGT-6, and PBA-5/PPGT-6. The UCST of PBA-240/PPGT-6, PBA-42/PPGT-6, and PBA-5/PPGT-6 are 339, 294, and 243 K, respectively. Using the reference molecular weight for PPG, the number of the F−H units in PPGT-6 becomes 67. Then the interaction parameter for PBA/PPGT-6 blends was estimated from the data for PBA-240/PPGT-6 and PBA-42/PPGT-6 on the basis of eqs 2−4. The constants α and β were determined to be −0.027 and +13, respectively. For the sake of later discussion, we calculated T_c and ϕ_c of several blends which were used in the calorimetry and dielectric measurements. The results are listed in Table 3. We also calculated the cloud point curves of PBA-21/PPGD-3 and PBA-21/PPGT-6 and are shown in Figures 2 and 3 by the dashed lines.

We found that the χ parameter for blends composed of linear PPGD-3 is higher than those of star-shaped PPGT-6. This indicates that star-shaped PPG is more easily mixed with PBA than linear PPG. Because of the stereo hindrance around the junction point of the star-shaped PPG molecules, the PBA chains cannot penetrate into the center of the star-shaped PPG molecules.

Table 3. Volume Fraction ϕ_c and Temperature T_c at Critical Point[a]

blend	ϕ_c	T_c
PBA-240/PPGD-3	0.10	280
PBA-42/PPGD-3	0.26	261
PBA-21/PPGD-3	(0.31)	(246)
PBA-3/PPGD-3	(0.54)	(176)
PBA-380/PPGT-6	(0.13)	(344)
PBA-245/PPGT-6	0.13	337
PBA-42/PPGT-6	0.27	295
PBA-21/PPGT-6	(0.39)	(265)
PBA-5/PPGT-6	0.45 ± 0.1	220 ± 10
PBA-3/PPGT-6	(0.63)	(150)

[a] Parentheses indicate the calculated value.

Such a hindrance causes decrease of the number of contacts between the PBA and PPG segments.

This idea was already proposed by Faust et al.,[19] who reported that the cloud point curves for a blend of linear polystyrene (PS) and linear poly(vinyl methyl ether) (PVME) and that of star-shaped PS and PVME are superposable if the composition ϕ of PS of the blend of star-shaped PS and PVME is multiplied by a factor $1 - k$ ($k \sim 0.35$). To explain this result, they considered that since the monomer concentration is very high in the core of the 22-arm star, the neighboring molecules will not be able to penetrate into the star center. Thus, 35% of the segments of the star PS are screened from interacting with the segments of PVME.

In the F−H theory (eq 1) the mixing entropy term was derived by assuming that n_1 and n_2 moles polymers 1 and 2 are arranged on the lattice sites randomly, and therefore the entropy term will not change much if there exist screened regions. On the other hand, the enthalpy term is effective only for the unscreened segments. Therefore, the enthalpy term of eq 1 is rewritten as $(1 - k)\chi\phi_1\phi_2$ where χ is the interaction parameter for the blends of linear components. The terms α and β/T of χ represent the entropy and enthalpy change due to the interaction of the segments. As mentioned above, the value of β for PBA/PPGD was 27 while that for PBA/PPGT was 13. From these data k for PBA/PPGT blends becomes 0.52. This surprisingly high factor of the screened fraction is an overestimate and is probably due to the mean field approximation of the F−H theory. A more rigorous approach is needed to determine the fraction of the screened region. Here we compare the difference between the blends studied by Faust et al.[19] and those used in this study. Faust et al. used blends of high molecular weight star-shaped PS with 22 arms and PVME. The molecular weight of PS was 1.28×10^6 and that of PVME 9.9×10^4. In the present study the molecular weight M_w of PPGT was ca. 6000, and the number of arms is three. Comparing them, we see that despite more than 2 orders difference in M_w, the screening factors are of the same order.

Glass Transition of Blends. Figure 4 shows the thermograms of differential scanning calorimetry (DSC) for the PBA/PPG blends. The composition of all blends used for DSC measurements was 50/50. For all runs, measurements were carried out at the heating rate of 5 K/min after samples were cooled at ca. −5 K/min. We defined T_g as the temperature at which the change of the DSC curve was steepest. Runs 1 and 2 show the DSC curves for pure PBA-380 and PPGT-6, respectively. For PBA-380, T_g is determined to be 222 K, and for PPGT-6 T_g is 201 K. Run 3 shows the DSC curve of a blend of PBA-380/PPGT-6. This blend has the cloud

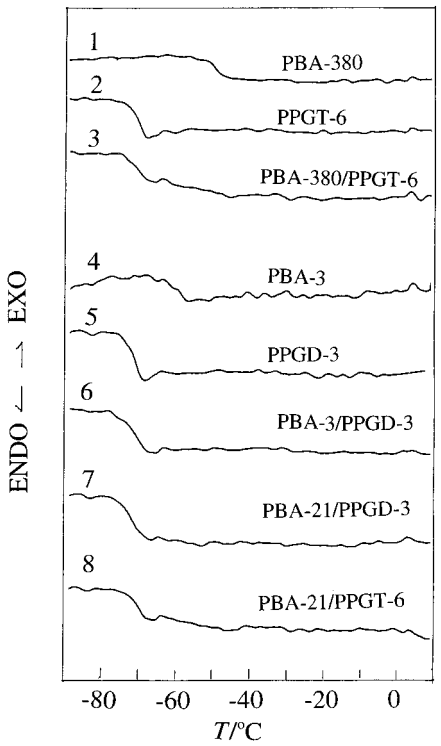

Figure 4. DSC thermograms of PBA, PPG, and blends of PBA/PPG: (1) PBA-380; (2) PPGT-6; (3) PBA-380/PPGT-6(50/50); (4) PBA-3; (5) PPGD-3; (6) PBA-3/PPGD-3(50/50); (7) PBA-21/PPGD-3(50/50); (8) PBA-21/PPGT-6(50/50).

point at about 320 K and is in the phase-separated state. In run 3, we see a relatively sharp change of the heat capacity at $T_g = 200$ K and a broad glass transition over 205−225 K. Obviously, the former corresponds to T_g of the PPGT-6-rich phase and the latter the PBA-rich phase. In contrast to our expectation, the T_g of the PBA-rich phase is not sharp, indicating that the phase contains some amount of PPGT-6 and that distribution of the composition is broad. From the phase diagram shown in Figure 3 and the F−H theory, the PPG-rich phase is almost pure PPGT-6, but the PBA-rich phase contains ca. 10% of PPGT-6 in the temperature range 200−250 K. As the origin of this broad T_g for the PBA-rich phase, one may consider a kinetic effect, that the rate of phase separation is so slow that the phase is not in the equilibrium state in the cooling process. To test this possibility, we measured the DSC curve for the same sample when cooled slowly at the rate of −1 K/min and annealed at 240 K for 1 h. However, the DSC diagram was not changed by this heat treatment. Therefore, the kinetic effect can be ruled out.

In connection with this result, we note that for blends in which the degree of polymerization of PBA (x_1) is much higher than that of PPG (x_2) the Flory−Huggins theory predicts that the PBA-rich phase contains a substantial amount of PPG, but the PPG phase is almost pure. Therefore, in PBA-380/PPGT-6 blends, the PBA-380-rich phase can accommodate PPGT-6, but the PPGT-6-rich phase is almost pure PPGT-6. The broad T_g of the PBA-rich phase indicates that there exists concentration fluctuation in the PBA-rich phase as suggested above.

Runs 4, 5, and 6 show the DSC diagrams of PBA-3, PPGD-3, and a blend of PBA-3/PPGD-3 (50/50), respectively. From these diagrams we determined the T_g's of PBA-3, PPGD-3, and PBA-3/PPGD-3 to be 211, 201, and

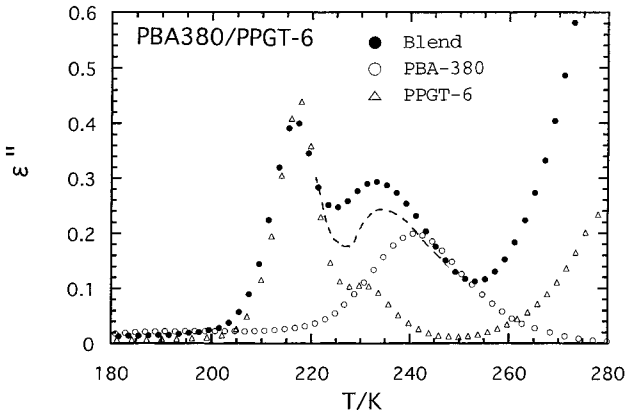

Figure 5. Temperature dependence curves of the dielectric constant ϵ' and loss factor ϵ'' for PBA-380/PPGT-6(50/50) and the ϵ'' multiplied by $^1/_2$ for the components PBA-380 and PPGT-6.

203 K, respectively. In contrast to run 3 for the PBA-380/PPGT-6 blend, the blend of PBA-3/PPGD-3 shows a single sharp glass transition. From the χ parameter, the cloud point of this system T_c of PBA-3/PPGD-3 is calculated to be 181 K. Therefore, at about 200 K this phase is in a mixed state. For mixtures of polymers such as random copolymers, various mixing rules of T_g have been proposed.[27−29] It is seen that T_g of the blend is close to that of PPGD-3. In the present blends, the difference of T_g's of the components is too small to test these blending rules.

Runs 7 and 8 show the DSC diagrams for PBA-21/PPGD-3 (50/50) and PBA-21/PPGT-6 (50/50), respectively. Although not shown in this figure, the DSC diagram of PBA-21 is close to that of PBA-380 and T_g of PBA-21 is 225 K. From the phase behavior, the cloud points of the former and the latter are estimated to be 240 and 262 K, respectively. Thus, below 240 K these blends are in the phase-separated state. However, as is seen in Figure 4, T_g's of both blends are 200−203 K and are relatively sharp as for a mixed blend of PBA-3/PPGD-3 (run 6). For the test of the kinetic effect on phase separation, the blends were annealed at 230 K for 1 h and then cooled below 200 K, but the DSC diagrams were the same as those cooled at −5 K/min. Therefore, the apparently single T_g of these blends is not due to the kinetic effect. Here we recall that PBA-380/PPBT-6 (run 3) exhibited broad T_g of the PBA-rich phase. Probably this trend has been enhanced in runs 7 and 8 since the cloud points of these blends are close to the T_g. Thus, we can regard that these blends are in weakly phase-separated states. Since the glass transition is due to cooperative segmental motions of long range, a heterogeneity of composition of relatively short length scale is not reflected on the glass transition. In this sense the DSC method is not sensitive to detect the effects of the phase separation.

Dielectric Relaxation. Figure 5 compares the temperature dependencies of dielectric loss factor ϵ'' at 100 Hz for PBA-380, PPGT-6, and 50/50 blend of PBA-380/PPGT-6. In this figure we plotted ϵ'' of PBA-380 and PPGT-6 multiplied by $^1/_2$ since the blend is the 50/50 mixture. First we look at the behavior of the pure components. In the ϵ'' curve of PPGT-6 shown in Figure 5, a small shoulder can be seen at 230 K. This shoulder is assigned to the normal mode relaxation due to fluctuation of the end-to-end vector.[22−24] On the other hand, PBA-380 exhibits a single peak at 242 K due to the segmental mode.

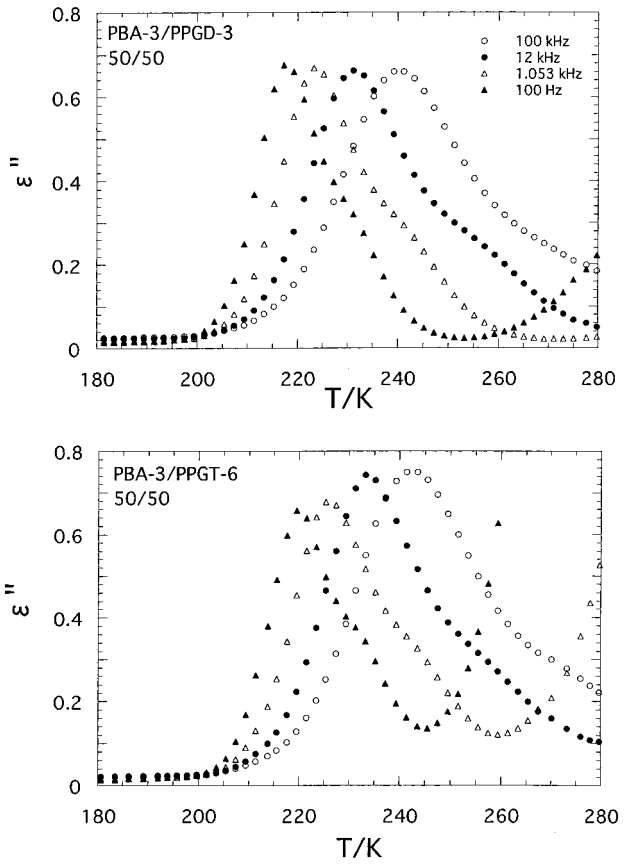

Figure 6. Temperature dependence curves of the dielectric loss factor ϵ'' at 100 Hz, 1 kHz, 12 kHz, and 100 kHz for (top) PBA-3/PPGD-3(50/50) and (bottom) PBA-3/PBGT-6.

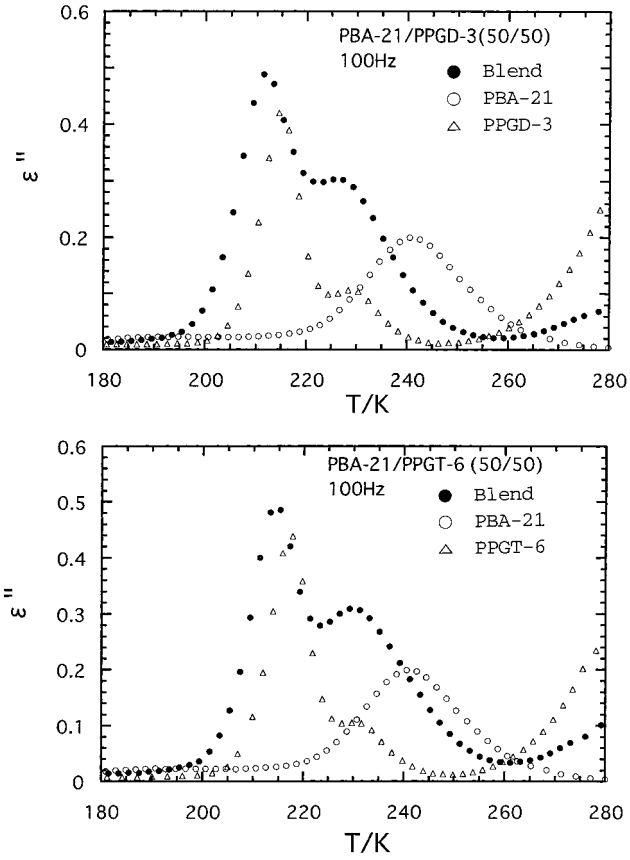

Figure 7. Temperature dependence curves of the dielectric loss factor ϵ'' for (top) PBA-21/PPGD-3(50/50) and the $\epsilon''/2$ of PBA-21 and PPGD-3 and (bottom) PBA-21/PPGT-6(50/50) and the $\epsilon''/2$ of PBA-21 and PPGD-3.

For PBA-380/PPGT-6 blend two peaks can be seen at about 218 and 232 K. As mentioned for the DSC thermogram, the cloud point of this blend is 320 K, and therefore the blend is in a phase-separated state. The low-temperature and high-temperature peaks are due to the PPG-rich and PBA-rich phases, respectively. For demixed blends, the additivity rule of the dielectric constant depends on the morphology of the blend. As is discussed in part 2 of this series,[30] we simply assume that the ϵ'' curve of a blend ϵ_b'' is given by the weighted sum of the components 1 and 2:

$$\epsilon_b'' = w_1\epsilon_1'' + w_2\epsilon_2'' \qquad (5)$$

where w_1 and w_2 are the composition of the components in wt/vol. The dashed line in Figure 5 shows the ϵ'' curve given by eq 5. We see that the observed high-temperature peak is at a lower temperature side than the one calculated with eq 5. In addition, the high-temperature peak is broad compared with the low-temperature peak. This is consistent with the DSC observation.

Figure 6 shows the temperature dependence curves of ϵ'' for a mixed blends of PBA-3/PPGD-3(50/50) and PBA-3/PPGT-6 (50/50). The loss curves are composed of a main peak and a shoulder in the high-temperature side. Judging from the location and intensity of the shoulder, we can assign the shoulder to the normal mode relaxation of PPGD-3. The height of the main peak is 0.65. This value is close to the sum of the contributions of the components; i.e., the peak height for the segmental mode of PPG is 0.43, and that for PBA is 0.2. Therefore, the loss peak of these blends can be assigned to a peak in which the peaks of the PBA-3 and PPGD-3 are merged. If the contribution of the normal mode of PPG is subtracted from the observed ϵ'' curve, the remaining peak due to the segmental mode is asymmetrical and is extended on the high-temperature side. This suggests that the relaxations due to the PBA segments locates at higher temperature than those of PPG-3. This indicates that there exists local heterogeneity even in a thermodynamically mixed state. In the discussion on the phase behavior, we speculated that half of the PPGT-6 segments locating around the center of the molecule are not mixed with the PBA segments in mixed blends. If this is the case, the ϵ'' curve for the blend of PPGT-6 would exhibit the ϵ'' curve in which the high- and low-temperature peaks are more clearly resolved compared with that of blends of linear PPGD-3. In Figure 6, we cannot see such a difference. Therefore, the dielectric data indicate that the screening factor k obtained above is an overestimate.

Figure 7 compares the ϵ'' curves at 100 Hz of the blends of PBA-21/PPGD-3 (50/50) and PBA-21/PPGT-6 (50/50). In these figures we also plotted ϵ'' multiplied by $^1/_2$ for the components. The cloud points of these blends have been estimated to be 240 and 262 K, respectively. Thus, in the range below 260 K where the dielectric relaxation was observed, these blends are in a phase-separated state. We recall that the DSC thermograms for these blends exhibit a single T_g indicating the behavior for mixed blends. We see that the ϵ'' curves have shapes intermediate of those for the high molecular weight blend PBA-380/PPGT-6 (Figure 5) and low molecular weight blend PBA-3/PPGD-3 (Figure 6). It is apparent that the sums of the ϵ'' curves of the compo-

nents (eq 5) do not agree with the observed ϵ'' curves. In addition, the high-temperature peak is too strong to ascribe the peak to the normal mode of PPG. Therefore, these blends are considered to be in a weakly segregated state as discussed for the data of DSC, and the high-temperature peak can be assigned to the contributions of both the PBA-rich phase and the normal mode of PPG. Comparing the ϵ'' curves of PBA-21/PPGD-3 and PBA-21/PPGT-6 blends, we see that the latter exhibits a more clearly separated high-temperature peak than that for PBA-21/PPGD-3. This behavior is consistent with the fact that the latter has higher cloud points than the former.

Conclusion

We have reported the phase diagram, glass transition temperatures T_g, and dielectric relaxation of PBA/PPG blends. The phase diagrams were of the upper critical solution type (UCST), and the critical temperatures T_c ranged from 200 to 330 K depending on the molecular weight of PBA. The phase behavior for blends composed of PBA and linear PPG was found to be different from those composed of PBA and star-shaped PPG. The difference has been explained by assuming that the segments locating around the center of the star-shaped PPG do not contact with the PBA segments due to steric hindrance. This speculation is not in harmony with the dielectric behavior. For blends of high molecular weight PBA-380 and PPG, two glass transitions were observed by DSC measurements. On the other hand, a mixed blend composed of low molecular weight PBA-3 and PPG exhibited a single T_g. For blends PBA-21/PPG whose T_g located near the cloud points, the thermograms exhibited single T_g, but the ϵ'' curves were bimodal. We have speculated that these blends are in a weakly segregated state. The shape of the dielectric ϵ'' curves of a blend in the mixed state was asymmetrical. We have concluded that even above the cloud point the segments of PBA and PPG are not perfectly mixed in the length scale of the segments.

References and Notes

(1) *Polymer Blends*; Paul, D. R., Newman, S., Eds.; Academic: Orlando, FL, 1978.
(2) Olabisi, O.; Robeson, L. M.; Shaw, M. T. *Polymer−Polymer Miscibility*; Academic: Orlando, FL, 1979; Chapter 3, pp 117−193 and references cited therein.
(3) Bank, M.; Leffingwell, J.; Thies, C. *Macromolecules* **1971**, *4*, 32.
(4) Yang, H.; Ricci, S.; Collins, M. *Macromolecules* **1991**, *24*, 5128.
(5) Bank, M.; Leffinwell, J.; Thies, C. *J. Polym. Sci., Part A-2* **1972**, *10*, 1097.
(6) Cheng, Y. W.; Stein, R. S. *Macromolecules* **1994**, *27*, 2512.
(7) Konigsveld, R.; Kleintjens, L. A. *J. Polym. Sci., Polym. Symp.* **1977**, *61*, 221.
(8) Han, C. D.; Chun, S. B.; Hahn, S. T.; Harpa, S. Q.; Savickas, P. J.; Meunier, D. M.; Li, L.; Yalcin, T. *Macromolecules* **1998**, *31*, 394.
(9) Shaw, M. T. *J. Appl. Polym. Sci.* **1974**, *18*, 449.
(10) Kelts, L. W.; Landry, C. J. T.; Teegarden, D. M. *Macromolecules* **1993**, *26*, 2941.
(11) Kwek, K. D.; Okada, M.; Chiba, T.; Nose, T. *Macromolecules* **1992**, *25*, 7204.
(12) Runt, J. P. Dielectric Studies of Polymer Blends. In *Dielectric Spectroscopy of Polymerc Materials*; Runt, J. P., Fitzgerald, J. J., Eds.; American Chemical Society: Washington, DC, 1997; Chapter 10, pp 283−302.
(13) Rellick, G. S.; Runt, J. *J. Polym. Sci., Polym. Phys. Ed.* **1986**, *24*, 313.
(14) Wetton, A. G.; MacKnight, W. J.; Fried, J. R.; Karasz, F. E. *Macromolecules* **1978**, *11*, 158.
(15) Katana, G.; Fischer, E. W.; Hack, Th.; Abetz, V.; Kremer, F. *Macromolecules* **1995**, *28*, 2714.
(16) Alegria, A.; Colmenero, C. M.; Ngai, K. L.; Roland, C. M. *Macromolecules* **1994**, *27*, 4486.
(17) Se, K.; Takayanagi, O.; Adachi, K. *Macromolecules* **1997**, *30*, 4877.
(18) Nishi, T.; Wang, T. T.; Kwei, T. K. *Macromolecules* **1975**, *8*, 227.
(19) Faust, A. B.; Sremcich, P. S.; Gilmer, J. W.; Mays, J. W. *Macromolecules* **1989**, *22*, 1250.
(20) Flory, P. J. *J. Chem. Phys.* **1941**, *9*, 660.
(21) Huggins, M. L. *J. Chem. Phys.* **1941**, *9*, 440.
(22) Stockmayer, W. H. *Pure Appl. Chem.* **1967**, *15*, 539.
(23) Baur, M. E.; Stockmayer, W. H. *J. Chem. Phys.* **1965**, *41*, 4311.
(24) Stockmayer, W. H.; Burke, J. J. *Macromolecules* **1969**, *2*, 647.
(25) Adachi, K.; Kotaka, T. *Prog. Polym. Sci.* **1993**, *18*, 585.
(26) Imanishi, Y.; Adachi, K.; Kotaka, T. *J. Chem. Phys.* **1988**, *89*, 7585.
(27) Fox, T. G. *Bull. Am. Phys. Soc.* **1956**, *1*, 123.
(28) DiMarzio, E. A.; Gibbs, J. H. *J. Polym. Sci.* **1963**, *A1*, 1417.
(29) Kwei, T. K. *J. Polym. Sci., Polym. Sci. Lett. Ed.* **1984**, *22*, 307.
(30) Hayakawa, T.; Adachi, K. *Macromolecules* **2000**, *33*, 6840.

MA000684V